Ab Initio Modeling of Boron Clustering in Silicon

Wolfgang Windl*, Xiang-Yang Liu**, and Michael P. Masquelier**

* Digital DNA Laboratories, Motorola, Inc., MD K20, 3501 Ed Bluestein Blvd, Austin, TX 78721
** Computational Materials Group, Motorola, Inc., MS B285, Los Alamos, NM 87545

ABSTRACT

We present results of *ab initio* calculations for the structure and energetics of boron-interstitial clusters in Si and a respective continuum model for the nucleation, growth, and dissolution of such clusters. The structure of the clusters and their possible relationship to boron precipitates and interstitial-cluster formation are discussed. Our continuum model suggest that inclusion of the fractional activation of charged clusters into the overall carrier count can make a substantial difference, if a sample contains a large fraction of B clustered in B_3I^- clusters, which might present a way to probe these clusters experimentally.

Keywords: Ab initio, boron clustering, deactivation, multiscale process modeling

1 INTRODUCTION

Ion implantation is currently the method of choice for introducing dopants such as boron into silicon. [1] However, energetic ions damage the host material and create a supersaturation of defects in Si, which impair the device performance. Annealing following the implant is used to heal the implant damage, while activating the dopant atoms electrically at the same time. The implant-anneal cycle can cause excessive transient enhanced diffusion (TED) of the implanted B and the formation of B precipitates which immobilize and deactivate the B atoms well below the solid solubility limit. [2] From the observation of the trapping of interstitials (Is) by these precipitates, [3] it was concluded that they consist of B-I clusters (BICs).

A notable body of simulation work in order to model these effects exists, [4]–[9] which all are based on the clustering energetics of the BICs. Two different approaches have been chosen to determine these energetics: First, an inverse-modeling fit of the BIC energies to a large set of secondary-ion mass spectroscopy (SIMS) measurements. [8] However, fitting a large number of parameters in inverse modeling can be subject to ambiguities and furthermore does not help to identify the structure of the clusters. The second approach, atomistic calculations, especially within density-functional theory (DFT), [9]–[15] can in principle overcome these limitations; however, the problems to find global instead of local minima [16] and the possibly considerable error bars for miscoordinated defects [17] also require a cautious use of this approach. Until recently, only one set of BIC reaction barriers from first-principles [18] for B_nI_m ($n \leq 4$) clusters had been available, where the influence of the different charge states had been neglected. Very recently, revised energetics from a new study which has been performed in parallel to our work have been published by the same group, [9], [14] after indications had been found that the previous numbers could not explain all experiments: In Ref. [7], several of the cluster energies of Ref. [18] had to be re-fitted in order to predict annealing experiments correctly. Also, the predictions of Ref. [4], based on the cluster energies of Ref. [18], where an "activation window" for B anneals was predicted, have been shown recently not to be in agreement with experiment. [19]

We present in this paper a systematic study of BIC energetics and structures including the influence of charges and a careful structure minimization within the BIC phase space. Also, we discuss the considerable differences between the results within the local-density approximation (LDA) and the generalized-gradient approximation (GGA). We compare our results to the other calculations and to the inverse-modeling results of Ref. [8], and finally discuss the influence of charge state and electronic structure of the BICs on device characteristics.

2 METHOD

For our calculations, we used the DFT code VASP with ultrasoft pseudopotentials within both LDA and GGA. [20] We employed a harder variation of the B pseudopotential with a cut-off energy of 230 eV and 64-atom supercells with a 4^3 Monkhorst-Pack k-point sampling. Testing a few clusters (BI^+, B_2I^0, B_3I^-, and $B_{12}I_7^=$) within 216-atom supercells, we find the finite-size error in the calculated energy state for the 64-atom cells to be reasonably small, up to a few tenths of an eV or $\sim$ 7%. The procedure to calculate energies for charged systems and the total-energy corrections for occupied defect states are identical to the ones described in Ref. [12].

We examined a number of BICs B_nI_m with $n, m \leq 4$,

Computational Nanoscience 2001, (www.cr.org), ISBN 0-9708275-3-9.

as well as $B_{12}I_7$, which has been studied theoretically in the past without presenting formation energy values, [21] and single B atoms in {311} defects. As pointed out before, [16] it is not clear in advance which final atomic arrangement the different clusters will assume in the global-minimum structure. In order to decrease the threat of finding a high-energy local instead of the global minimum, we started for each cluster from many different initial configurations that were structurally relaxed (including previously predicted ones from Refs. [10], [11], [16]). Further details will be published elsewhere. [22]

3 B CLUSTERING

3.1 Ab Initio Results

Figure 1 summarizes our first-principles results. For all examined clusters (except for $B_4^{=}$ and B-{311}) we show the structure, LDA, and GGA energy as well as the fitted energies of Ref. [8]. The reference states for the cluster binding energy $E_{\rm cl}$ are B^- and I^0. For B_nI_m,

$$E_{\rm cl} = E_{B_nI_m} - n(E_{B^-} - E_{Si}) - m(E_{I^0} - E_{Si}) - E_{Si},$$

where the bulk Si cell has N atoms, and B_nI_m has $N+m$ atoms in the supercell. This is supposedly the same way the cluster energies in Ref. [8] are defined. We show the most stable structures and energies we could find for the lowest-energy charge states at mid gap and leave a more detailed discussion of the Fermi-level dependence for later. [22] In contrast to the tight-binding results [16] and the inverse modeling [8], we find for all-substitutional B clusters repulsive energies (0.9, $\sim$ 2.2, and $\sim$ 2.5 eV for $B_2^{=}$, B_3^{3-}, and $B_4^{=}$, respectively), making the existence of such clusters highly improbable. All other clusters have negative formation energy, in contrast to the tight-binding calculations of Ref. [16], which furthermore predicts different structures for most of the examined clusters. Stripping band gap and monopole corrections from our LDA numbers, we find mostly reasonable agreement with the numbers of Ref. [14], deviating between 3 and 40% and on average 15%. These differences, in conjunction with the different levels of corrections, add up to large differences in most of the reaction barriers between our work and Ref. [14], up to more than 1 eV.

The systematic of the structural clustering process can be best seen by comparing clusters with identical I number and differing B content. For one I, the structure does not depend on the number of electrons (which is identical for all B_nI clusters), but strongly on the number of B atoms: for BI^+, we find a tetrahedral Si interstitial; for B_2I^0, we confirm the previously found ⟨100⟩ B dumbbell; [10], [11] for B_3I^-, we find a bond-centered B interstitial between the two other B atoms; and for $B_4I^=$, we calculate a 16° tilted ⟨100⟩ dumbbell between the two other B atoms. For BICs involving

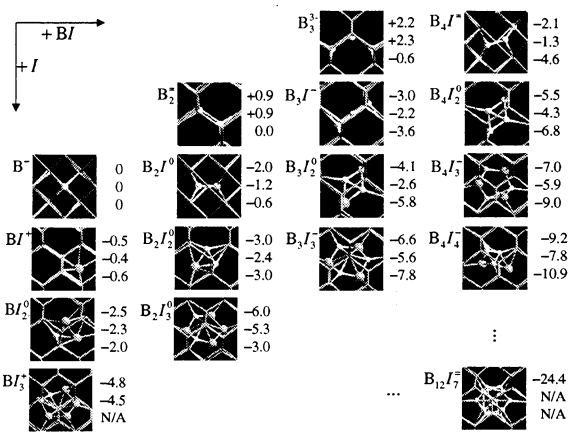

Figure 1: Structure and energetics of the considered BICs (except B_4 and B-{311}). The small white balls are B atoms, the large gray balls are Si atoms involved in the cluster. All other Si atom are shown as a stick-only network. The energy values (eV) next to each picture are, top to down, energies within GGA, LDA, and the fitted values from Ref. [8].

two Is, the clusters contain triangular shapes; triangles form the surface of icosahedra, which form the structure of pure B. For B_nI_3, we find six-membered rings in the $(2\bar{3}\bar{3})$ plane, which could be the starting point for channel-like interstitial clusters. Pure phases of channel structures, so-called silisils, have been predicted several years ago. [23] Small units of such silisils, embedded into bulk diamond-type Si, are believed to form the rod-like {311} interstitial clusters. [24] Therefore, growth seems to be possible towards both icosahedral and {311} structures, with B possibly encouraging ring growth: for perfect Si, the I_3 ring which to our knowledge has not been reported previously, has an $\sim$ 0.2 eV higher energy than more compact structures [25]. B addition makes the ring the most stable structure which therefore might result in enhanced {311} growth. Larger clusters which could support this suggestion are becoming less feasible because of an exceeding number of degrees of freedom. However, we studied two possible border cases for the two mechanisms: One is a B icosahedron, $B_{12}I_7^{=}$, embedded into Si, which has been suggested before. [21] There, we find because of the nearly perfect bonding and small strain, a very low energy state with an extremely high binding energy of 3.5 eV per I. Therefore, even though the clustering path is not clear, it seems that such "bulk B"-like clusters might be very stable I traps in high-B concentration regions, which is supported by experiments. [26] The other case is a B atom in an infinite {311} extended defect, whose role had been ruled negligible in Ref. [8]. Indeed, we find a binding energy of a mobile BI pair [12] nearly identical to that of a free I, suggesting that {311} clusters exert no special

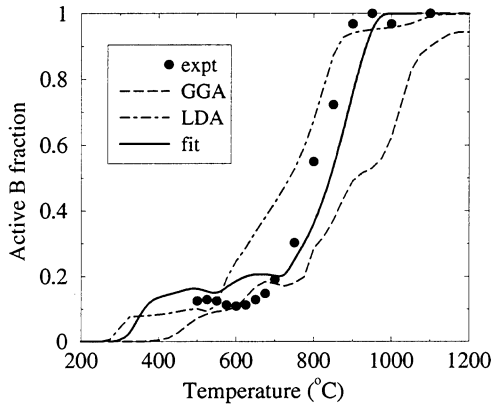

Figure 2: Simulated and experimental B activation after a 40 keV, 2e14 cm^{-3} B implant for 30-min anneals at varying temperatures, assuming only substitutional, unclustered B to be active. Dashed line: LDA clustering energies; dot-dashed line: GGA energies; solid line: fit as explained in the text. The circles represent experimental values from Ref. [19].

attractive/repulsive influence on migrating B. However, we did not calculate the interaction of several B atoms in {311}s, which could change the energetics strongly, similar to moving one substitutional B atom from a bulk position to a $B_2I_3^0$ cluster, which we find to lower the energy by nearly 1 eV (Fig. 1).

3.2 Continuum Results

We implemented the clustering model from Fig. 1 (excluding $B_{12}I_7$ and B-{311}) into a continuum model, combined with a well-tested four-stream model for intrinsic B diffusion including the B migration mechanism from Ref. [12] and mostly *ab initio* calculated point-defect energetics and prefactors from Ref. [27]. For I clustering, we mainly use the model from Ref. [28]. We first assume only substitutional B^- to be electrically active and all clustered B to be deactivated. The results for B activation are shown in Fig. 2. Both LDA and GGA models correctly predict inverse annealing at low temperatures due to the beginning formation of B_3I^- and $B_4I_2^0$ whose importance has also been discussed in previous work. [5], [4], [8], [9] Due to the very low energy that we find for $B_2I_3^0$, however, we find in contrast to previous work that also the decay of this high-I content cluster contributes significantly to the activation process at higher temperatures (Fig. 3).

LDA predicts too much activation too soon, whereas GGA results in too strong clustering as compared to experiment. In order to improve agreement with experiment, we used a Genetic Algorithm [29] to re-fit the parameters to a large number of SIMS data for different annealing conditions. [30] The fit result was mostly independent of the starting parameters and resulted in

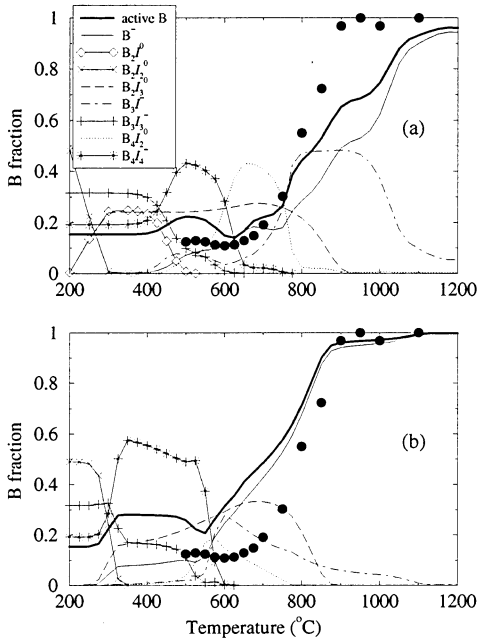

Figure 3: (a) GGA and (b) LDA result for the fraction of B atoms trapped in the different clusters. All clusters are shown whose maximum fraction is higher than 0.05. The active B sums up all holes provided by the substitutional and clustered B. Experimental points are from Ref. [19].

parameter values which lay with a few exceptions between the LDA and GGA values, which therefore might be considered as upper and lower boundaries for the clustering energies. No activation data were used for the fit, and still, the experimental data in Fig. 2 are well reproduced by this model.

We want to point out that despite the fact that GGA and LDA predict somehow comparable energies and activation behavior in Fig. 2, the clustering paths are substantially different. This is shown in Fig. 3, where besides the overall activation, also the evolution of B atoms trapped in the different clusters is given. Whereas for GGA [Fig. 3(a)] the B_3I^- cluster dominates the late stage of the activation process, it is a combination of B_3I^-, $B_4I_2^0$, and especially $B_2I_3^0$ for LDA [Fig. 3(b)]; our fit (not shown) on the other hand finds a strong preference for $B_4I_2^0$.

Overall, the major features of our model are in agreement with those of the calibration-only approach of Ref. [8] (initial formation of high-I content clusters; later emission of Is, resulting in low-I content clusters). However, we find that pure B clusters without Is have forbiddingly high energy and that $B_2I_3^0$ should be a third key-cluster besides B_3I^- and $B_4I_2^0$, in contrast to the findings of Ref. [8].

4 BAND STRUCTURES

The purpose of doping Si with acceptors (group-III elements) and donors (group-V elements) is to create excess holes and electrons and thus change the conductivity of the host material. "Shallow acceptors" such as B can be easily understood within a simple hydrogenic theory on grounds of the Coulomb potential of the charged dopant. [31] In principle, one expects the introduction of B into Si to create an acceptor band about 45 meV above the valence band edge. However, this very shallow band is not resolved in our calculation and hybridizes with the valence bands of the Si host material. This should be due to the fact that our 64-atom periodic cell with a B-B distance of 10.9 Å is much smaller than the exciton wave function of the shallow state which can be estimated to extend up to $a^* = \varepsilon_0 \, (m/m^*) \, a_B \simeq 42$ Å for light holes (ε_0 is the dielectric constant and (m/m^*) the effective hole mass in Si; a_B is the Bohr radius). [32] The result [Fig. 4(b)] is a band structure for substitutional B nearly identical to the one for perfect Si [Fig. 4(a)]. The hole that the B atom provides can be seen from the fact that the Fermi level for the neutral B system drops under the valence band edge, providing room for an extra electron.

If the BICs would maintain the B atoms' property of providing holes in the valence band, their appearance would not affect the electrical characteristics of the device dramatically. Indeed, there are BICs like the icosahedral $B_{12}I_7$ structure that provide room for extra electrons, while still maintaining an overall band structure without bands deep inside the gap [Fig. 4(d)]. However, we can tell from the position of the Fermi level (which results in the minimum charge state of 2−) that only two holes are induced by this cluster. This means that 10 B atoms in the cluster do not provide holes and thus have been deactivated. Such BICs are therefore only "fractionally" active.

In order to examine the influence of the fractional activation of the BICs on the overall conductivity, we show in Fig. 3 two different approaches to model the ratio of introduced holes over the inserted B atoms: One is the model from Sec. 3.2, where we assume that only substitutional, unclustered B^- atoms provide single holes to the system. The other one assumes that also charged clusters contribute to the carrier pool, with one hole provided for every electron captured. As an example, the B_3I^- cluster provides one hole for its three clustered B atoms. Figure 3 shows that all models predict B_3I^- to be the only charged cluster prevalent at temperatures relevant to applications. Depending on its abundance, the total number of holes can be significantly different from the number of substitutional B atoms. This might provide a possibility to probe the occurrence of B_3I^- clusters experimentally by a combination of SIMS, SRP, and sheet-resistance measurements.

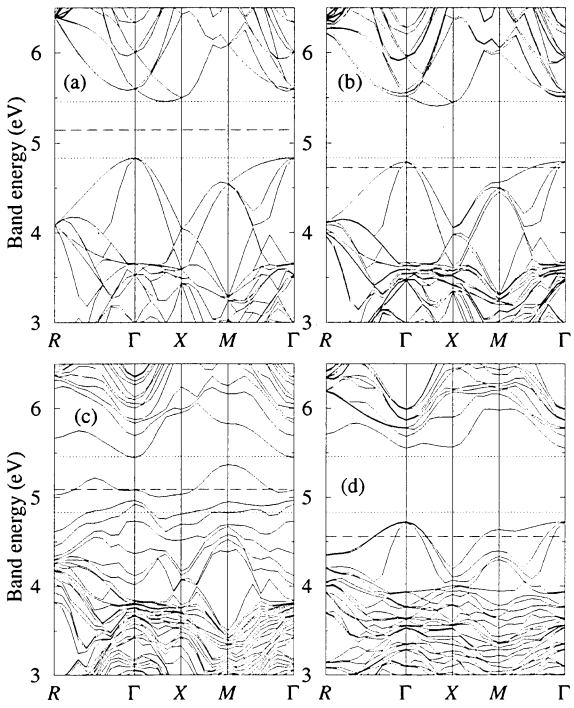

Figure 4: Band structure of (a) perfect Si, (b) a substitutional B^0 atom, (c) a BI_2^0 cluster, and (d) a B icosahedron $B_{12}I_7^0$ in a 64-atom Si supercell. The long-dashed line is the Fermi level, and the dotted lines represent valence and conduction band edges of perfect Si.

Many of the cluster bandstructures display isolated states deep inside the gap regime [see, e.g., Fig. 4(c)] which can cause leakage currents in device structures. However, it is difficult to discuss these states or use them as input to device simulations for two reasons: Due to our supercell approximation, where a "large" piece of Si is repeated periodically because of computational reasons, these localized states can interact with the ones in neighboring cells, resulting in dispersion of the otherwise flat band. Furthermore, within LDA and GGA, the band gap in Si is considerably underestimated to be about half the experimental value [Fig. 4(a)]. Since deep states are often atomic-like states which are caused by the difference in the on-site potential, [33] their position relative to the LDA/GGA gap cannot be describe by a simple scaling or shifting operation, making the uncertainty as big as the gap energy. More sophisticated methods to overcome this problem involving more advanced approximations for the exchange-correlation potential are currently the subject of ongoing research. [34]

5 SUMMARY

In summary, we presented results of *ab-initio* calculations for the structure and energetics of BICs in Si

and a continuum model for the nucleation, growth, and dissolution of such clusters. We showed that neither LDA nor GGA compare perfectly well to experimental annealing and activation studies. However, gentle re-fitting of the numbers results in a model with good predictive quality. Concerning the electronic states, our simulations suggest that inclusion of the fractional activation of charged clusters into the overall carrier count can make a substantial difference, if a sample contains a large fraction of B clustered in B_3I^- clusters.

6 ACKNOWLEDGMENTS

We would like to thank Keith Beardmore, Iuval Clejan, Alex Demkov, Murray Daw, Dejan Jovanovic, and Roland Stumpf for very helpful interactions.

REFERENCES

[1] E. Chason, S. T. Picraux, J. M. Poate, J. O. Borland, M. I. Current, T. Diaz de la Rubia, D. J. Eaglesham, O. W. Holland, M. E. Law, C. W. Magee, J. W. Mayer, J. Melngailis, and A. F. Tasch, J. Appl. Phys. **81**, 6513 (1997).

[2] P. A. Stolk, H.-J. Gossmann, D. J. Eaglesham, D. C. Jacobson, and J. M. Poate, Appl. Phys. Lett. **66**, 568 (1995); L. H. Zhang, K. S. Jones, P. H. Chi, and D. S. Simons, *ibid.* **67**, 2025 (1995).

[3] T. E. Haynes, D. J. Eaglesham, P. A. Stolk, H.-J. Gossmann, D. C. Jacobson, and J. M. Poate, Appl. Phys. Lett. **69**, 1376 (1996).

[4] M. J. Caturla, M. D. Johnson, and T. Diaz de la Rubia, Appl. Phys. Lett. **72**, 2736 (1998).

[5] A. D. Lilak, S. K. Earles, K. S. Jones, M. E. Law, and M. D. Giles, Tech. Dig. Int. Electron Devices Meet., 493 (1997).

[6] M. M. Bunea and S. T. Dunham, Mater. Res. Soc. Symp. Proc. **490**, 3 (1998).

[7] D. Stiebel, P. Pichler, and H. Ryssel, Mater. Res. Soc. Symp. Proc. **538**, 141 (1999).

[8] L. Pelaz, G. H. Gilmer, H.-J. Gossmann, and C. S. Rafferty, Appl. Phys. Lett. **74**, 3657 (1999).

[9] S. K. Theiss, M. J. Caturla, M. D. Johnson, J. Zhu, T. Lenosky, B. Sadigh, and T. Diaz de la Rubia, Thin Solid Films **365**, 219 (2000).

[10] E. Tarnow, J. Phys. Condens. Matter **4**, 5405 (1992).

[11] J. Zhu, T. Diaz de la Rubia, L. H. Yang, C. Mailhiot, and G. H. Gilmer, Phys. Rev. B **54**, 4741 (1996).

[12] W. Windl, M. M. Bunea, R. Stumpf, S. T. Dunham, and M. P. Masquelier, in *Proc. of the 2nd International Conference on Modeling and Simulation of Microsystems, April 19-21, 1999, San Juan, Puerto Rico* (Computational Publications, Cambridge, MA 1999), p. 369; Mater. Res. Soc. Symp. Proc. **568**, 91 (1999); Phys. Rev. Lett. **83**, 4345 (1999).

[13] B. Sadigh, T. J. Lenosky, S. K. Theiss, M. J. Caturla, T. Diaz de la Rubia, and M. A. Foad, Phys. Rev. Lett. **83**, 4341 (1999).

[14] T. J. Lenosky, B. Sadigh, S. K. Theiss, M. J. Caturla, and T. Diaz de la Rubia, Appl. Phys. Lett. **77**, 1834 (2000).

[15] X.-Y. Liu, W. Windl, and M. P. Masquelier, Appl. Phys. Lett. **77**, 2018 (2000).

[16] W. Luo, P. B. Rasband, P. Clancy, and B. W. Roberts, J. Appl. Phys. **84**, 2476 (1998).

[17] W.-K. Leung, R. J. Needs, G. Rajagopal, S. Itoh, and S. Ihara, Phys. Rev. Lett. **83**, 2351 (1999).

[18] J. Zhu (unpublished); partially reported in Ref. [4].

[19] A. Mokhberi, P. Griffin, and J. D. Plummer (unpublished).

[20] G. Kresse and J. Hafner, Phys. Rev. B **47**, 558 (1993); **49**, 14 251 (1994); J. Phys.: Condens. Matter **6**, 8245 (1994); G. Kresse and J. Furthmüller, Comput. Mater. Sci. **6**, 15 (1996); Phys. Rev. B **55**, 11 169 (1996).

[21] J. Yamauchi, N. Aoki, and I. Mizushima, Phys. Rev. B **55**, 10 245 (1997).

[22] X.-Y. Liu, W. Windl, and M. P. Masquelier (unpublished).

[23] A. A. Demkov, W. Windl, and O. F. Sankey, Phys. Rev. B **53**, 11 288 (1996).

[24] J. Kim, J. W. Wilkins, F. S. Khan, and A. Canning, Phys. Rev. B **55**, 16 186 (1997).

[25] J. Kim, F. Kirchhoff, J. W. Wilkins, and F. S. Khan, Phys. Rev. Lett. **84**, 503 (2000).

[26] I. Mizushima, M. Watanabe, A. Murakoshi, M. Hotta, M. Kashiwagi, M. Yoshiki, Appl. Phys. Lett. **63**, 373 (1993); I. Mizushima, A. Murakoshi, M. Watanabe, M. Yoshiki, M. Hotta, M. Kashiwagi, Jpn. J. Appl. Phys. 1 **33**, 404 (1994).

[27] B. P. Uberuaga, W. Windl, R. Stumpf, and H. Jónsson (unpublished).

[28] C. S. Rafferty, G. H. Gilmer, M. Jaraiz, D. Eaglesham, and H.-J. Gossmann, Appl. Phys. Lett. **68**, 2395 (1996).

[29] P. Mazumder and E. M. Rudnick, *Genetic Algorithms for VLSI Design, Layout and Test Automation* (Prentice Hall, Upper Saddle River, NJ, 1999).

[30] M. P. Rendon and I. Clejan (unpublished).

[31] P. Y. Yu and M. Cardona, *Fundamentals of Semiconductors* (Springer, Berlin, 1996), pp. 150.

[32] W. Windl and A. A. Demkov, Mater. Res. Soc. Symp. Proc. **510**, 181 (1998).

[33] W. Windl, O. F. Sankey, and J. Menéndez, Phys. Rev. B **57**, 2431 (1998).

[34] See, e.g., B. P. Uberuaga, H. Jónsson, R. Stumpf, and W. Windl (to be published).